CHAPTER III

EVALUATION OF A "FLOATING" AEROBICS FLOOR

3.1 Description of Laboratory Test Floor

The "floating" aerobics floor concept was tested at the Structures and Materials Laboratory at Virginia Polytechnic Institute and State University in Blacksburg, Virginia. The following sections describe the lateral restraint system, air spring assembly, and initial testing procedures.

3.1.1 Lateral Restraint System

The pneumatic air springs supporting the floor slab have no lateral stability when inflated; therefore, a lateral restraint system was developed to allow unrestricted vertical movement with as little lateral movement as possible.

After several unsuccessful attempts to restrain the lateral movement of the floor slab, lateral bracing was determined to be the best solution. The bracing scheme is shown in Figure 3.1 and consists of several components. Two 1-1/4 in. hollow square steel bars, or "arms", with eye bolts threaded into each end were connected to a 2 in. hollow square steel center bar on one end and mounting plates bolted to stub columns on the opposite ends.

To attach the eye bolts in the ends of the "arms" to the center bar and stub column mounting plates, a 5/8 in. x 2 in. bolt was placed in each eye of the eye bolts. The bolts were placed in a hole in the end of the center bar or stub column mounting plate and secured with a washer and nut. The center bar was mounted to the floor slab with a 5/8 in. threaded rod through its center and the stub columns were bolted to the reaction floor with 7/8 in. x 3 in. bolts.

The lateral bracing system allowed movement in the vertical direction but restrained lateral movement in the direction perpendicular to the longitudinal axis of the center bar. The orientation of the center bar was rotated by extending or retracting the threaded eye bolts in the ends of the "arms". One set of lateral bracing was attached to each corner of the slab and the orientation was alternated to restrict as much lateral movement as possible. The results listed in this report were all obtained using the lateral bracing system.

3.1.2 Air Spring Assembly

Each air spring was attached to a mounting plate with two bolts as shown in Figure 2.2. The triangular access holes allowed access to the mounting bolts and the air spring air inlet assembly.

The inlet air assembly, consisted of 1/4 in. x 6 in. brass pipe nipple threaded into the air spring. The pipe nipple extended above the level of the floor slab allowing for the attachment of a pressure gauge, air release ball valve, air inlet valve, and 1/2 in. inside diameter (i.d.) rubber tubing. The pressure gauge was attached to a 1/4 in. galvanized tee fitting which was connected to the pipe nipple. Each of the additional components were attached to a 3/8 in. cross fitting which was threaded onto a 1/4 in. x 1 in. galvanized pipe nipple connected to the tee fitting. The rubber tubing was approximately 4 ft. in length and was attached to a 5 gallon air storage tank.

The air storage tank was equipped with an air inlet valve assembly, which was threaded into the top of the tank. Adjustment of the air inlet valve modified the damping in the system by controlling the air flow in and out of the tank.

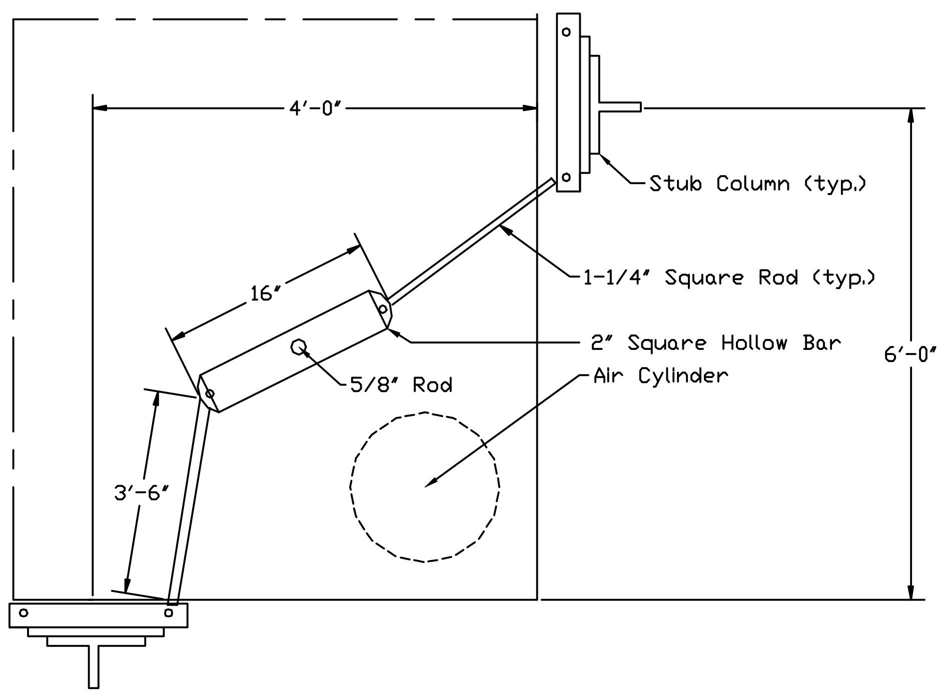

a) Plan View

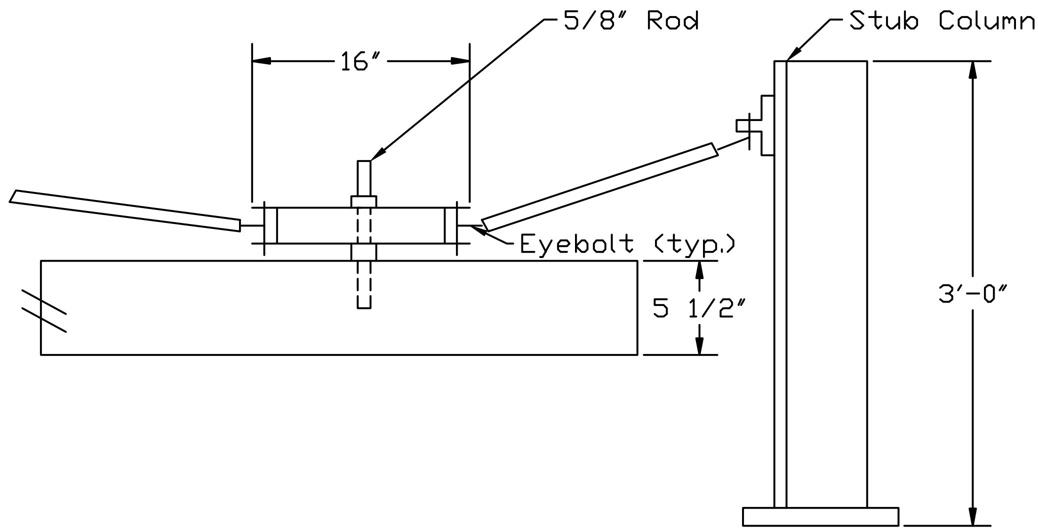

b) Elevation View (Air spring assembly not shown for clarity)

Figure 3.1 Lateral Bracing Typical Corner Details

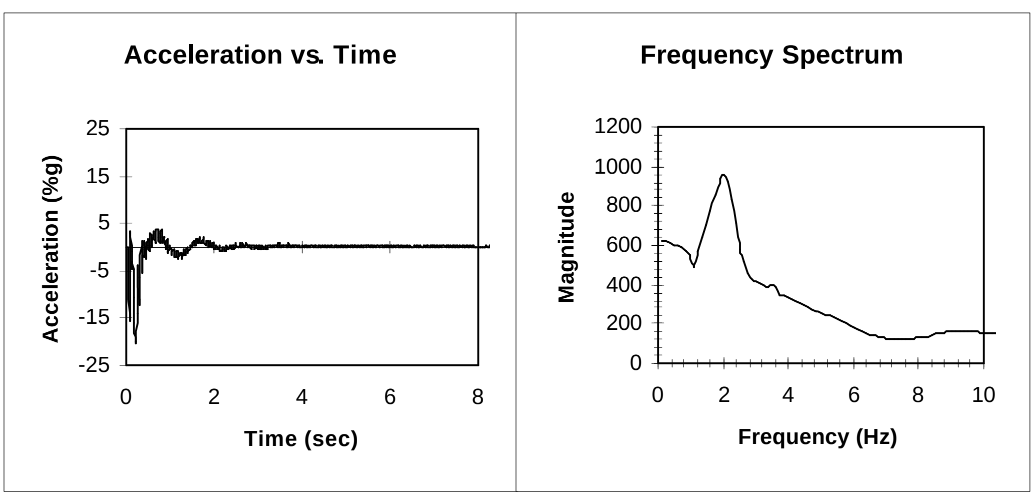

Figure 3.2 Typical Acceleration Response and Frequency Spectrum of Initial Floor Configuration - Valves Connected in a Loop

3.1.3 Initial Testing

After the floor system was stabilized on the laboratory reaction floor, initial tests were performed to determine the vibration characteristics of the system. The air springs were connected in a loop with 3/8 in. (inside diameter) rubber tubing. The loop of tubing was connected to one 5 gallon air storage tank.

The air springs were inflated to the design height of 15 in. and internal pressure of 40 psi. Natural frequencies between 1.6 hz and 2.0 hz were measured for this set-up. These natural frequencies fall within the range of 1.5 hz to 3.0 hz, which are typical frequencies of aerobics music. Therefore, this floor set-up was unacceptable because a resonance condition could occur during slower exercises. A typical acceleration response and corresponding frequency spectrum due to HDS impact are shown in Figure 3.2.

The air spring pressure was increased and decreased from the design pressure of 40 psi, with little change in the natural frequency. Additional weight was added to the floor slab by means of four 60 lb. concrete blocks stacked at each corner. By increasing the mass of the floor, the natural frequency would be reduced. However, measurements showed that the addition of the concrete blocks had little effect on the natural frequency of the system.

To reduce the natural frequency of the air springs, the floor system was reconfigured with air storage tanks attached directly to each air spring. The tubing diameter was increased to 1/2 in. (inside diameter) to decrease the damping and non-linearity of the system. By increasing the tubing diameter, the air flowing in and out of the air spring contacted more surface area inside the tubing. The rate of the air flow was reduced, which reduced the damping in the system.

During the initial testing of the reconfigured tubing system, the design natural frequency of 1.19 hz of the air springs listed in the Firestone Design Catalog was not achieved. A natural frequency of 1.5 hz was measured due to heel drop excitation. A possible cause of the higher natural frequency was attributed to the restriction of the air flow by the 1/8 in. diameter orifice in the air valve assembly. By restricting the air flow, additional stiffness was developed in the spring due to the pressure build-up.

To resolve the problem, the air inlet valve assembly was removed and the rubber tubing was attached directly to the air tank. The removal of the valve assembly reduced the natural frequency to an acceptable level of 1.06 hz. The test results are summarized later in this chapter.

After the desired natural frequency was achieved during the initial testing, further tests were performed to determine the damping characteristics and force transmission of the floor system. Removing the air inlet valve assembly lowered the natural frequency from the values obtained with the air inlet valve assembly installed in the air tanks, but it was not apparent whether the peak acceleration magnitude and percentage of force transmission to the supporting floor was also reduced. To determine that the floor configuration with the air inlet valve assembly removed was the most favorable in terms of lowest natural frequency, peak acceleration magnitude, and percentage of force transmission to the supporting floor, a comparison of three valve configurations was performed.

Three air inlet valve configurations were tested: (1) open valve, (2) closed valve, and (3) no valve. The measured results in this report are based on the three valve configurations and are shown in the following sections as a means of comparison.

3.2 Vibration Characteristics

3.2.1 Natural Frequency

3.2.1.1 Vertical Mode of Oscillation

The measured natural frequency for the vertical mode of oscillation was determined for each valve configuration. The HDS, resting on the force plate, and the accelerometer were placed at the center of the floor slab. The HDS was used to impact the floor ten times and the corresponding acceleration and force input traces were recorded (Figure 3.3). An FFT of each acceleration response was obtained and the peak magnitude and corresponding frequency were recorded. The FFTs of the ten floor excitations by the HDS were averaged to determine the natural frequency of the vertical mode of oscillation of the system, which is assumed to be the frequency at the highest peak of the frequency response.

In a similar manner, the measured frequency of the output force to the ground floor for the vertical mode of oscillation was determined. The floor system was deflated and the force plate was removed from under the HDS and placed under one of the air springs. The floor was re-inflated and ten additional impacts of the HDS were performed. The resulting acceleration response at the center of the floor and the output force response to the ground floor were recorded.

The FFTs of the output force responses were averaged and the peak magnitude and corresponding natural frequency were determined. The natural frequencies were identical to the frequencies for the floor slab in the vertical mode of oscillation and are listed in Table 3.1.

The predicted natural frequency of the vertical mode of oscillation was obtained from Equation (2.1) using SDOF theory. The spring constant, k, is 395 lb/in. and the effective mass of the floor in the vertical mode is 3015 lb. The results are listed in Table 3.2 and sample calculations are shown in Appendix A.

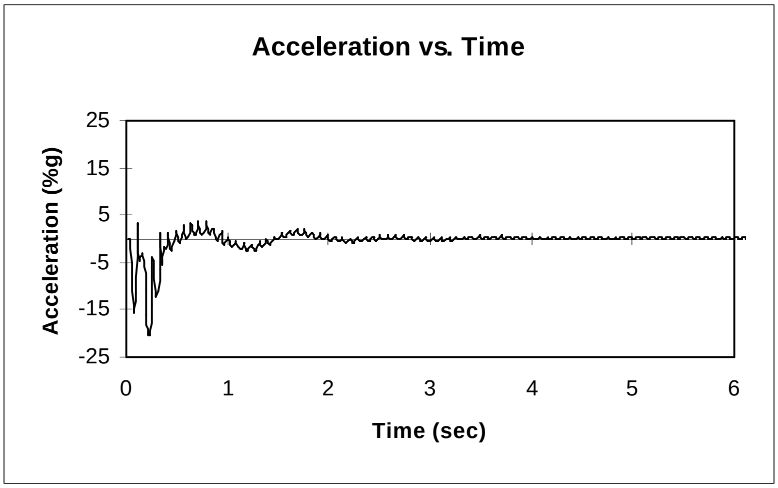

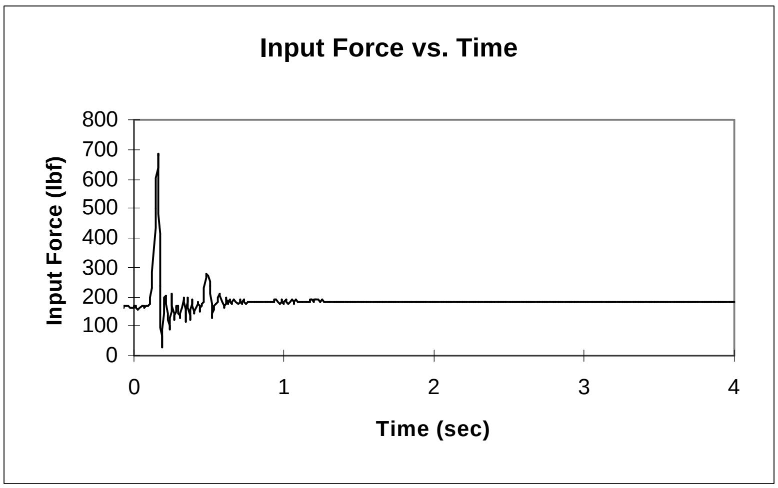

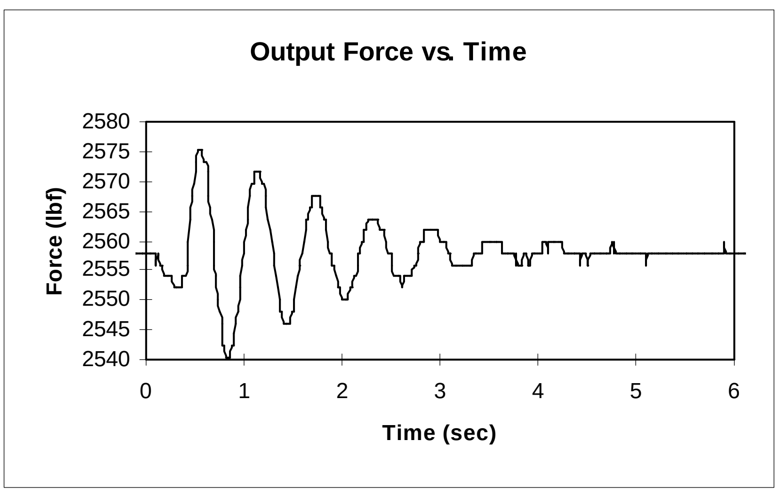

Figure 3.3 Typical Acceleration, Input Force, and Output Force Response Due to HDS Impact at Center of Slab

3.2.1.2 Corner and Side Rotating Modes of Oscillation

The measured natural frequency of the corner rotating mode of oscillation was determined using the HDS and accelerometer at opposite 1/4 points, as shown in Figure 2.7. An FFT analysis was performed on the acceleration response and the natural frequencies were determined from peaks on the frequency response. Several impacts of the HDS were performed but only one response was recorded after the results were found to be consistent.

In a similar manner, the measured natural frequency of the side rotating mode of oscillation was determined by placing the HDS and accelerometer on opposite sides of the floor slab, as shown in Figure 2.8. The results are shown in Table 3.1.

The predicted natural frequency of the corner and side rotating modes of oscillation were determined using approximate and exact analyses. The results are shown in Table 3.2 and sample calculations for the predicted natural frequencies are shown in Appendix A.

Table 3.1 Measured Natural Frequencies

Valve Position	**Damping Ratio (%)**	**Mode of Oscillation** Measured Natural Frequency (Hz)		
		Vertical	**Corner Rotation**	**Side Rotation**
No Valve	5.2	1.0625	1.4375	1.4375
Open Valve	10.1	1.125	1.5625	1.5625
Closed Valve	5.0	1.375	1.875	1.875

Table 3.2 Predicted Natural Frequencies

Valve Position	**Mode of Oscillation** Predicted Natural Frequency (Hz)				
	Vertical	**Corner Rotation**		**Side Rotation**	
		Approx. Solution	Exact Solution	Approx. Solution	Exact Solution
No Valve	1.13	1.68	1.58	1.57	1.58
Open Valve	1.13	1.68	1.58	1.57	1.58
Closed Valve	1.13	1.68	1.58	1.57	1.58

3.2.2 Damping Ratio

The damping ratio, or percentage of critical damping, of the floor system was determined using the logarithmic decrement method described in Chapter 2. The input acceleration responses from the ten HDS impacts utilized to determine the natural frequency of the floor system in the vertical mode of oscillation were used to determine a damping ratio.

The first five cycles of the acceleration response were used and logarithmic decrement and damping ratio values were obtained for each acceleration response. The damping ratios shown in Table 3.1 are the average values of for each valve configuration to determine the damping ratio of the system. Sample calculations are shown in Appendix A.

3.2.3 Acceleration Response

The measured acceleration response of the floor system due to steady-state jumping excitation was converted from the recorded voltage to a value expressed in %g. The level of acceleration at the first harmonic due to one 160 lb man jumping at the center of the floor at 1.5, 2.0, 2.5, and 3.0 hz is shown in Table 3.3.

The measured acceleration level at the second harmonic was determined by multiplying the measured level at the first harmonic by the ratio of the magnitudes of the frequency response at the second harmonic to the first harmonic. In a similar manner, the acceleration level at the third harmonic was determined (Allen 1997). The ratios between the first, second, and third harmonics are shown in Table 3.3 and the peak acceleration results are shown in Table 3.4. Sample calculations are shown in Appendix A.

The predicted peak acceleration response due to four participants was determined by multiplying the peak acceleration value for one person jumping by four, as described in Chapter 2. The predicted results are shown in Table 3.4.

Table 3.3 Ratio of FFT Magnitudes Determined from Acceleration Response

		Ratio of FFT Magnitudes from Acceleration Response	
Valve Position	**Jumping Frequency (Hz)**	**Second to First Harmonic**	**Third to First Harmonic**
None	1.5	0.14	0.13
	2.0	0.18	0.02
	2.5	0.31	0.04
	3.0	0.47	0.06
Open	1.5	0.08	0.07
	2.0	0.15	0.01
	2.5	0.17	0.05
	3.0	0.34	0.04
Closed	1.5	0.09	0.05
	2.0	0.18	0.01
	2.5	0.25	0.03
	3.0	0.39	0.04

Table 3.4 Measured and Predicted Acceleration Response

		Peak Acceleration (%g)					
Valve Position	**Jumping Frequency (Hz)**	**First Harmonic**		**Second Harmonic**		**Third Harmonic**	
		1 Jumper (Meas.)	4 Jumper (Pred.)	1 Jumper (Meas.)	4 Jumper (Pred.)	1 Jumper (Meas.)	4 Jumper (Pred.)
None	1.5	2.24	8.96	0.32	1.28	0.29	1.16
	2.0	2.30	9.20	0.42	1.68	0.05	0.20
	2.5	2.31	9.24	0.72	2.88	0.10	0.40
	3.0	2.31	9.24	1.09	4.36	0.13	0.52
Open	1.5	3.98	15.92	0.33	1.32	0.26	1.04
	2.0	3.18	12.72	0.49	1.96	0.05	0.20
	2.5	2.78	11.12	0.49	1.96	0.04	0.16
	3.0	2.90	11.60	0.98	3.92	0.13	0.52
Closed	1.5	4.81	19.24	0.44	1.76	0.24	0.96
	2.0	3.25	13.00	0.59	2.36	0.04	0.16
	2.5	3.08	12.32	0.78	3.12	0.09	0.36
	3.0	2.48	9.92	0.98	3.92	0.10	0.40

3.3 Force Transmission

The measured force transmission was determined based on steady-state jumping excitation of the floor system as described in Chapter 2. The percentage of the input force transmitted to the ground floor to an output force at the first harmonic was determined based on experimental results of jumping excitation at 1.5, 2.0, 2.5, and 3.0 hz. The ratios of the second and third harmonics to the first harmonic input and output forces, determined from FFTs, are shown in Tables 3.5 and 3.6 and the measured force results for the first harmonic are shown in Table 3.7.

Typical jumping acceleration and force response and corresponding frequency responses are shown in Figure 3.6. The acceleration and force responses for each valve configuration and jumping frequency are shown in Appendix B. The measured force transmission ratio was determined from the ratio of the magnitudes of the input force to the measured output force. The results are shown in Table 3.7 and sample calculations are shown in Appendix A.

The predicted force transmission was determined using Equation (2.7). The results for the predicted force transmission at the first harmonic are shown in Table 3.7 and sample calculations are shown in Appendix A.

The measured transmitted forces at the second harmonic were determined by multiplying the first harmonic input or output force by the ratio of the magnitude of the second harmonic to first harmonic forces in Table 3.5 and 3.6. The percentage of the input force transmitted to the ground was determined experimentally by the ratio of the measured input to measured output forces. The results are shown in Table 3.8 and sample calculations are shown in Appendix A.

In a similar manner, the transmitted forces at the third harmonic were determined. The results are shown in Table 3.9 and sample calculations are shown in Appendix A.

Table 3.5 Ratio of FFT Magnitudes Determined from Input Force Response

		Ratio of FFT Magnitudes Determined from Measured Input Force Response	
Valve Position	**Jumping Frequency (Hz)**	**Second to First Harmonic**	**Third to First Harmonic**
None	1.5	0.20	0.11
f_n = 1.06 hz	2.0	0.14	0.06
	2.5	0.16	0.01
	3.0	0.48	0.04
Open	1.5	0.21	0.12
f_n = 1.13 hz	2.0	0.28	0.02
	2.5	0.26	0.04
	3.0	0.34	0.05
Closed	1.5	0.22	0.16
f_n = 1.38 hz	2.0	0.22	0.05
	2.5	0.57	0.09
	3.0	0.25	0.03

Table 3.6 Ratio of FFT Magnitudes Determined from Output Force Response

		Ratio of FFT Magnitudes Determined from Measured Output Force Response	
Valve Position	**Jumping Frequency (Hz)**	**Second to First Harmonic**	**Third to First Harmonic**
None	1.5	0.04	0.03
	2.0	0.07	0.02
	2.5	0.22	0.02
	3.0	0.44	0.01
Open	1.5	0.03	0.01
	2.0	0.03	0.01
	2.5	0.07	0.01
	3.0	0.10	0.01
Closed	1.5	0.02	0.02
	2.0	0.05	0.01
	2.5	0.08	0.02
	3.0	0.12	0.01

Table 3.7 Measured and Predicted Force Transmission (First Harmonic)

Valve Position	Jumping Frequency (Hz)	Measured Input Force (lbf)	Measured Output Force (lbf)	Measured Force Trans. (%)	Predicted Force Trans. (%)	Ratio Measured/ Predicted
None	1.5	158.57	113.96	71.87	100.56	0.71
	2.0	212.31	51.72	24.36	45.46	0.54
	2.5	235.16	30.64	13.03	27.98	0.46
	3.0	257.34	26.48	10.29	19.86	0.52
Open	1.5	163.24	340.64	208.67	116.31	1.79
	2.0	233.16	161.60	69.31	58.57	1.18
	2.5	262.97	92.08	35.02	37.87	0.92
	3.0	267.54	61.76	23.08	27.86	0.83
Closed	1.5	160.81	428.84	266.67	317.93	0.84
	2.0	213.74	151.88	71.06	90.62	0.78
	2.5	286.09	104.48	36.52	46.54	0.78
	3.0	269.77	49.72	18.53	29.78	0.62

Table 3.8 Measured and Predicted Force Transmission (Second Harmonic)

Valve Position	Jumping Frequency (Hz)	Measured Input Force (lbf)	Measured Output Force (lbf)	Measured Force Trans. (%)	Predicted Force Trans. (%)	Ratio Measured/ Predicted
None	1.5	30.94	4.32	13.95	19.86	0.70
	2.0	30.15	3.66	12.14	12.41	0.98
	2.5	37.92	6.60	17.39	9.01	1.93
	3.0	124.72	11.69	9.38	7.09	1.32
Open	1.5	34.24	11.46	33.47	27.86	1.20
	2.0	64.33	4.78	7.43	18.30	0.41
	2.5	68.79	6.20	9.02	13.71	0.66
	3.0	90.84	6.15	6.77	11.01	0.61
Closed	1.5	35.25	7.42	21.06	29.78	0.71
	2.0	46.19	7.87	17.05	16.31	1.04
	2.5	161.91	8.75	5.41	10.87	0.50
	3.0	68.09	5.80	8.52	8.05	1.06

Table 3.9 Measured and Predicted Force Transmission (Third Harmonic)

Valve Position	Jumping Frequency (Hz)	Measured Input Force (lbf)	Measured Output Force (lbf)	Measured Force Trans. (%)	Predicted Force Trans. (%)	Ratio Measured/ Predicted
None	1.5	18.01	3.41	18.95	10.44	1.82
	2.0	13.26	0.84	6.36	7.09	0.90
	2.5	3.31	0.75	22.82	5.40	4.23
	3.0	10.26	0.26	2.56	4.37	0.59
Open	1.5	20.28	3.04	15.00	15.66	0.96
	2.0	5.06	1.22	24.08	11.01	2.19
	2.5	9.77	0.83	8.45	8.54	0.99
	3.0	13.91	0.66	4.72	7.00	0.67
Closed	1.5	24.96	9.33	37.38	13.09	2.86
	2.0	10.85	0.82	7.53	8.05	0.94
	2.5	25.45	1.86	7.30	5.75	1.27
	3.0	8.46	0.57	6.68	4.47	1.49

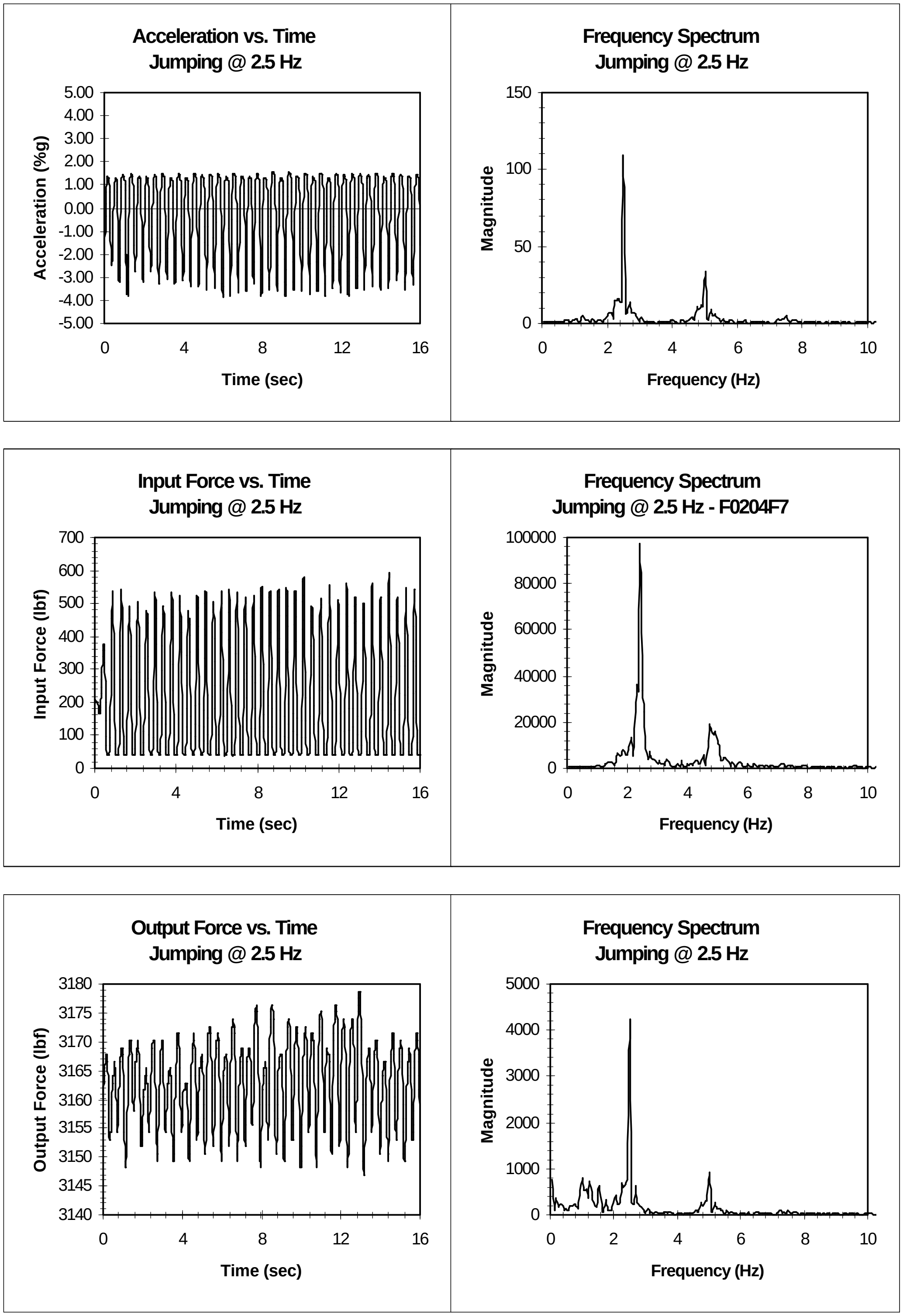

Figure 3.4 Typical Jumping Acceleration, Input, and Output Response

3.4 Acceptability Evaluations

Each valve configuration of the floor system was tested subjectively by experienced aerobicists to rate the "floating" floor acceptability in an actual installation. Three participants evaluated the floor. One person stood approximately 2 ft from one corner, while the other two participants performed two low impact aerobics steps and one high impact jump exercise at frequencies of 1.5, 2.0, 2.5, and 3.0 hz. Additionally, one person stood alone on the floor slab, while the other two participants stepped onto the floor and walked across the floor several times.

The closed valve configuration was reported to be unacceptable at all jumping frequencies, causing large amplitudes of motion and a "seasick" feeling to the person standing. The "seasick" feeling was a problem after the participants stopped jumping and stood motionless. Walking across the floor in this configuration caused unacceptable floor motion to the person standing as well as the people walking.

The open valve and no valve configurations were similar in the evaluation ratings. The high impact jumping exercises at 1.5 hz caused unacceptable motion to the person standing, while the participants did not experience unacceptable motion. At the higher frequencies, the motion was less perceptible. When all three participants simultaneously engaged in the jumping exercise, the floor motion was not perceptible to the standing person. The floor motion due to walking across the floor in these configurations was found to be similar to acceptable vibration levels felt in a standard floor system.